Annals of Biomedical Engineering, Vol. 32, No. 4, April 2004 (©2004) pp. 520–530

A Computational Tensegrity Model Predicts Dynamic Rheological Behaviors in Living Cells

CORNEL SULTAN,[1] DIMITRIJE STAMENOVIĆ,[2] and DONALD E. INGBER[1]

[1]Vascular Biology Program, Departments of Pathology and Surgery, Children's Hospital/Harvard Medical School, Boston, MA and [2]Department of Biomedical Engineering, Boston University, Boston, MA

(Received 30 July 2003; accepted 9 November 2003)

Abstract—Rheological properties of living cells play a key role in the control of cell shape, growth, movement, and contractility, yet little is known about how these properties are governed. Past approaches to understanding cell mechanics focused on the contributions of membranes, the viscous cytoplasm, and the individual filamentous biopolymers that are found within the cytoskeleton. In contrast, recent work has revealed that the dynamic mechanical behavior of cells depends on generic system properties, rather than on a single molecular property of the cell. In this paper, we show that a mathematical model of cell mechanics that depicts the intracellular cytoskeleton as a tensegrity structure composed of a prestressed network of interconnected microfilaments, microtubules, and intermediate filaments, and that has previously explained static cellular properties, also can predict fundamental dynamic behaviors of living cells.

Keywords—Tensegrity, Dynamics, Cell frequency response.

GLOSSARY

c = damping coefficient
l = length of a tendon (m)
l_0 = resting length of a tendon (m)
$\dot{\mathbf{r}}_n$ = velocity of the center of mass of the nth rigid body/point mass (m/s)
$\mathbf{q}$ = vector (24×1) of generalized coordinates
$\mathbf{q}_0$ = vector (24×1) of generalized coordinates at the reference solution
$\bar{\mathbf{q}}$ = perturbations vector (24×1) of independent generalized coordinates
z_1 = output perturbation
$\mathbf{A}(\mathbf{q})$ = equilibrium matrix (24×33)
$\mathbf{C}(\mathbf{q})$ = damping matrix (24×24)
$\mathbf{D}_0$ = output matrix (1×24)
EA = stiffness of a tendon (N)
$\mathbf{F}$ = vector ($N \times 1$) of external forces and torques
F_1 = input to the system
$\mathbf{F}_n$ = resultant force acting on the nth rigid body/point mass (N)
$\bar{\mathbf{F}}$ = vector ($N \times 1$) of perturbations in the external forces and torques
G' = elastic modulus (Pa)
G'' = frictional modulus (Pa)
$\mathbf{H}(\mathbf{q})$ = disturbance matrix ($24 \times N$)
$J(\omega, P)$ = transfer function
L = length of a strut (m)
$\mathbf{C}_0, \mathbf{K}_0, \mathbf{H}_0$ = damping, stiffness, and disturbance matrices, respectively, evaluated at $\mathbf{q}_0$
$\mathbf{M}_n$ = resultant moment acting on the nth rigid body (Nm)
N = number of external forces and torques applied to the structure
P = prestress (Pa)
Q_j = the jth nonconservative generalized force
T = force in a tendon (N)
$\mathbf{T}(\mathbf{q})$ = vector (33×1) of tensions in the working tendons
V = potential energy of the structure (J)
X_i, Y_i, Z_i = inertial Cartesian coordinates of the center of mass of strut i (m)
X, Y, Z = inertial Cartesian coordinates of the point mass (m)
Z_1 = output of the system
α_{ij} = azimuth angle of strut ij (°)
δ_{ij} = declination angle of strut ij (°)
ω = frequency (Hz)
$\mathbf{\Omega}_n$ = angular velocity of the nth rigid body (°/s)

INTRODUCTION

In standard *ad hoc* rheological models of the cell, the elastic and frictional stresses are assumed to originate from two distinct compartments—the elastic cortical membrane and the viscous cytoplasm.[40,12] More recent work suggests that cell rheological behavior reflects a generic property of the cell at some higher system level of molecular organization and interaction.[11] At the same time, it is well known that molecular filaments which comprise the intracellular solid state network known as the cytoskeleton (CSK), including

Address correspondence to Donald Ingber, MD, PhD, Vascular Biology Program, 11-128, New Research Building, Children's Hospital, 300 Longwood Avenue, Boston, MA 02115. Electronic mail: donald.ingber@tch.harvard.edu

microfilaments, microtubules, and intermediate filaments, play a central role in cell shape stability.[7–10,16,18,24,30,34,36] Thus, to advance our understanding of the molecular and biophysical basis of cell rheology, we must develop a theoretical model of the cell that both effectively predicts complex mechanical behaviors and provides a mechanism to link these behaviors to the molecular elements that comprise the CSK.

Tensegrity architecture provides a potential microstructural mechanism to explain the mechanical behavior of the cell.[16,17,29] The cellular tensegrity model assumes that contractile microfilaments and intermediate filaments carry a stabilizing tensile stress ("prestress") within the CSK that is balanced by internal microtubules and by extracellular adhesions. Thus, this model differs from continuum models of the cell in that it proposes a critical stabilizing role for CSK prestress in cell mechanics, and it predicts that specific molecular elements within the CSK elements will bear either tension or compression.

Mathematical formulations of tensegrity models, starting from first principles, have shown qualitative and quantitative consistencies with static experimental results in various cell types.[5,6,27–29,31,37,39] For example, in living airway smooth muscle cells stiffness increases nearly in proportion as the level of CSK contractile stress is raised,[36] a feature which is consistent with *a priori* predictions of the tensegrity model. It also has been shown that microtubules bear significant compressive forces in living cells,[30,36] much like the struts in tensegrity structures.[5,6,32]

One limitation of past work in this area is that all the above consistencies between tensegrity and the behaviors of living cells only reflect their static elastic properties. In contrast, numerous studies show that cell rheological behavior is viscoelastic.[2,9–11,13,22,25,26,30,33,35,40] The standard approach in modeling cell viscoelasticity is essentially phenomenological. For example, linear lumped spring-dashpot analogues are often used as basic models that are fit to the data obtained from mechanical measurements of living cells.[2,25,33] A more advanced model of this type includes a two-compartment model comprised of an elastic cortical membrane and a viscous or viscoelastic cytoplasm.[12,40] Although useful for quantitating cell viscoelastic parameters, these models do not take into account the existence of the internal CSK and its known role in bearing both static[24,25,30,34,36] and dynamic[2,11,13,22,26] mechanical loads within cells. Recently, Cañadas *et al.*[4] used a tensegrity structure with viscoelastic elements as a model of the CSK to analyze creep behavior of cells. We also previously used a stress-supported cable network model of the actin CSK, a structure organized upon similar principles as tensegrity, to analyze the effect of cell contractility upon elastic and frictional properties of the cell.[30] These models, however, only captured a limited number of features observed in cells, presumably because of oversimplification of modeling assumptions. In particular, these models failed to incorporate intermediate filaments that are known to play an important role in cell mechanics.[37]

Recent experimental studies revealed two fundamental, dynamic mechanical behaviors of cultured cells. First, at a given frequency of loading, both the elastic (storage) modulus (G') and frictional (loss) modulus (G'') increase approximately linearly with increasing contractile prestress in the CSK, with G' exhibiting a greater dependence.[30] Second, at a given prestress, both G' and G'' increase with increasing frequency according to a weak power-law[1,11,13] (power-law exponent $\sim$0.2). In the case of G', this power-law dependence extends over five decades of frequency[11] (10^{-2} to 10^{3} Hz). However, at very low frequencies $<10^{-2}$ Hz, G' has been reported to assume a constant value in certain cells.[13] G'' increases according to the same power-law up to 10 Hz, but at higher frequencies the power-law dependence increases and approaches unity at very high frequency, consistent with Newtonian viscous behavior.[1,11] In this study, we explored whether a computational model of tensegrity structures composed of simple viscoelastic members that represent intermediate filaments, as well as microfilaments and microtubules, could predict these dynamic behaviors that living cells exhibit during oscillatory loading.

MODEL

The tensegrity structure used in our model (Fig. 1) is composed of 3 struts, A_iC_i ($i = 1, 2, 3$) that attach to a fixed base through frictionless ball and socket joints; 3 struts, B_iD_i, that connect only to tendons; and 36 tendons that connect the end points of the struts. Of the 36 tendons, 12 that represent intermediate filaments are connected together to a point of negligible mass situated at the center of the structure (analogous to the nucleus of the cell), whereas the other 24 tendons that correspond to actin filaments connect to the end points of the struts (Fig. 1). The three tendons that connect the points of the base (A_1, A_2, A_3) are not important in our mathematical study because they connect fixed points, and thus, they do not influence the statics or dynamics of the structure. We call the other 33 tendons, working tendons. All struts, which represent microtubules or other compression-bearing elements of the CSK, are of identical length, L, in the model. The base triangle $A_1A_2A_3$ is equilateral with a side length $L\sqrt{3/8}$ (Fig. 1). It is assumed that the struts are rigid, of negligible thickness, and with negligible inertial properties. The tendons are assumed to be viscoelastic Voigt elements consisting of a linear elastic spring in parallel with a linear viscous damper. The constitutive equation of a tendon is

$$T = EA\left(\frac{l}{l_0} - 1\right) + c\dot{l}, \tag{1}$$

where T is the force, EA is the stiffness (defined as the product between the longitudinal modulus of elasticity, E, and the cross-sectional area, A, of a tendon), $c > 0$ is the

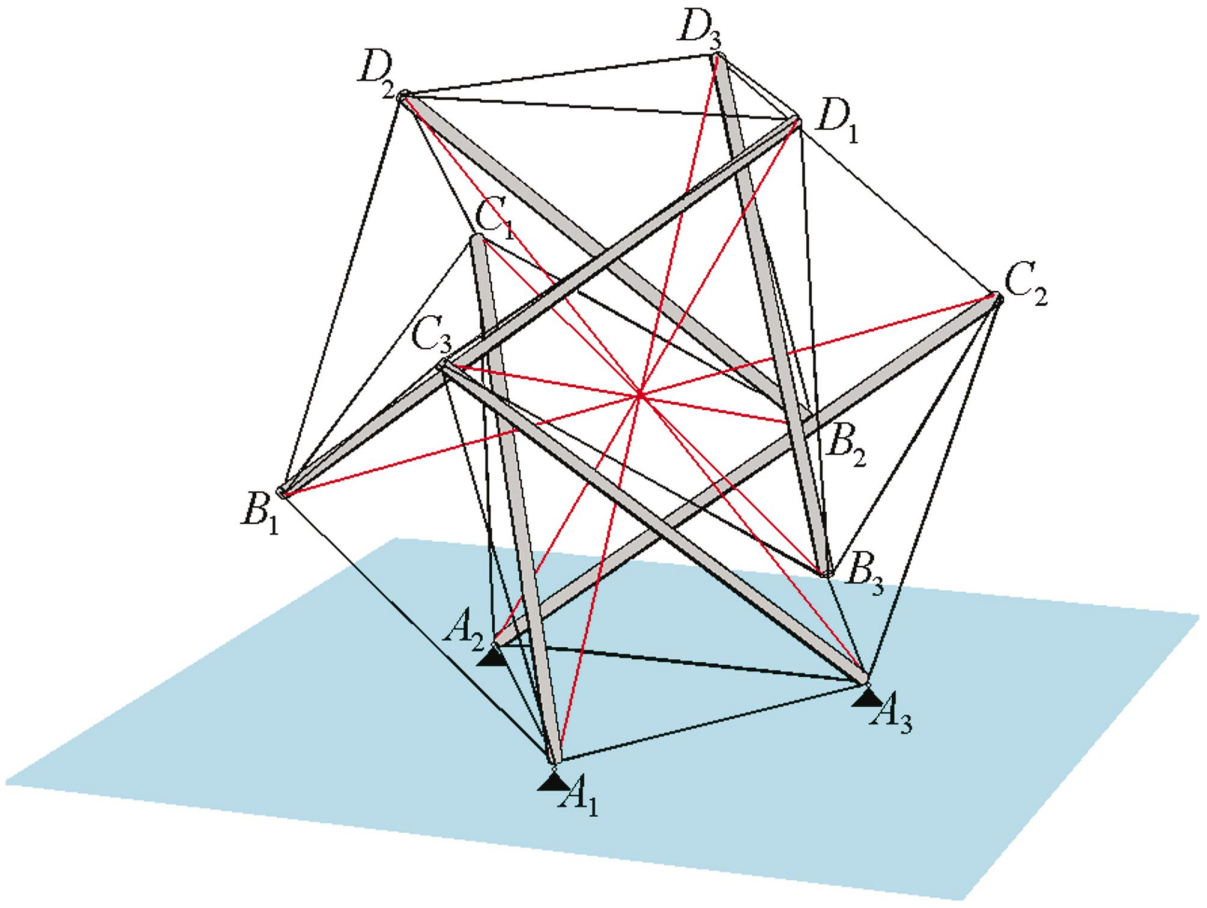

FIGURE 1. A spherical tensegrity structure with intermediate filaments used to generate the computational tensegrity model. The thin tendons represent microfilaments (black lines) and intermediate filaments (red lines); the thick gray struts indicate microtubules. Anchoring points to the substrate (blue) are indicated by the black triangles (A_1, A_2, and A_3).

damping coefficient, l and l_0 are the length and the resting length of the tendon, respectively, and the dot indicates the material time derivative.

For mathematical modeling, we introduced an inertial system of reference defined as follows: it is a right-handed system of orthonormal base vectors ($\mathbf{b}_1$, $\mathbf{b}_2$, $\mathbf{b}_3$) centered at the geometrical center of the base triangle, $A_1A_2A_3$, with $\mathbf{b}_1$ parallel to A_1A_3 and pointing toward A_3, and $\mathbf{b}_3$ perpendicular to the fixed plane $A_1A_2A_3$. The configuration of the structure is described by a set of independent generalized coordinates defined as follows. For each A_iC_i strut in Fig. 1, two angles are necessary and sufficient to specify its position: the azimuth, α_{i1}, and the declination, δ_{i1}, defined as follows: the declination is the angle between a strut and $\mathbf{b}_3$, and the azimuth the angle made by the orthogonal projection of the strut on $A_1A_2A_3$ and $\mathbf{b}_1$. For each B_iD_i strut in Fig. 1 in addition to the azimuth (α_{i2}) and declination (δ_{i2}) angles, the inertial Cartesian coordinates of its center of mass (X_i, Y_i, Z_i) are necessary. Finally, the point (without mass) at the center of the structure is characterized by its inertial Cartesian coordinates (X, Y, Z). The vector of generalized coordinates ($\mathbf{q}$) (24×1), obtained by assembling these independent generalized coordinates, is

$$\mathbf{q} = [\delta_{11}\,\alpha_{11}\,\delta_{21}\,\alpha_{21}\,\delta_{31}\,\alpha_{31}\,X_1\,Y_1\,Z_1\,\delta_{12}\,\alpha_{12}\;X_2\,Y_2\,Z_2\,\delta_{22}\,\alpha_{22}X_3\,Y_3\,Z_3\,\delta_{32}\,\alpha_{32}\,X\,Y\,Z]^T. \quad (2)$$

Equations of Motion

The equations of motion of the model were derived using the Lagrangean formulation. For this purpose, the potential energy and the nonconservative generalized forces acting on the structure were expressed in terms of the generalized coordinates. In this model we consider that the inertial properties of the structure (e.g., masses, moments of inertia of the struts) are negligible, hence the kinetic energy is 0. The potential energy (V) due to elasticity of the tendons was calculated using

$$V = 0.5\sum_{j=1}^{33} EA_j\left(\frac{l_j}{l_{0j}} - 1\right)^2, \quad (3)$$

where EA_j, l_j, and l_{0j} are the stiffness, length, and resting lengths, respectively, of the jth working tendon. The lengths of the tendons, l_j, were expressed in terms of the generalized coordinates, using simple geometry to derive the coordinates of the nodes of the structure and symbolic computational software (Maple) to compute the distances between these nodes.

The nonconservative forces acting on the structure (damping in the tendons, external forces on struts) result in a set of nonconservative generalized forces which were expressed using the principle of virtual work as:

$$Q_j = \sum_{n=1}^{7} \left(\mathbf{F}_n^T \frac{\partial \dot{\mathbf{r}}_n}{\partial \dot{q}_j} + \mathbf{M}_n^T \frac{\partial \boldsymbol{\Omega}_n}{\partial \dot{q}_j} \right), \tag{4}$$

where Q_j is the nonconservative generalized force associated with the jth generalized coordinate, q_j. Vectors $\mathbf{F}_n$, $\mathbf{M}_n$ are the resultant force and moment, respectively, acting on the nth rigid body (including the point mass), $\dot{\mathbf{r}}_n$ and $\boldsymbol{\Omega}_n$ are the velocity of the center of mass and angular velocity of the nth rigid body, respectively.

Lagrange equations are

$$\frac{\partial V}{\partial q_j} = Q_j, \qquad (j = 1, \ldots, 24). \tag{5}$$

Applied to this holonomic system they yielded

$$\mathbf{A}(\mathbf{q})\mathbf{T}(\mathbf{q}) + \mathbf{C}(\mathbf{q})\dot{\mathbf{q}} + \mathbf{H}(\mathbf{q})\mathbf{F} = \mathbf{0}, \tag{6}$$

where matrix function $\mathbf{A}(\mathbf{q})$ (24×33) is the equilibrium matrix, whose elements are:

$$\mathbf{A}_{ij} = \frac{\partial l_j}{\partial q_i} \quad (i = 1, \ldots, 24, \quad j = 1, \ldots, 33). \tag{7}$$

Vector function $\mathbf{T}(\mathbf{q})$ (33×1) indicates tensions in the working tendons. Matrix function $\mathbf{C}(\mathbf{q})$ (24×24) is the damping matrix, which is given as

$$\mathbf{C}(\mathbf{q}) = \sum_{j=1}^{33} c_j \mathbf{C}_j(\mathbf{q}), \tag{8}$$

where $\mathbf{C}_j(\mathbf{q})$ are matrices which depend on the geometric properties of the structure and c_j are damping coefficients of the working tendons. Matrix function $\mathbf{H}(\mathbf{q})$ is called the disturbance matrix, of size $(24 \times N)$, where N is the number of external forces and torques applied to the structure and assembled in the vector $\mathbf{F}$ $(N \times 1)$.

The derivation of these equations was carried out using symbolic computation under Maple. The resulting equations are too complicated to be given here. For frequency response calculations, the linearized equations of motion were derived from Eq. (6). Their derivation required the introduction of a reference solution of Eq. (6). In this study, we considered that the reference solution is a special equilibrium configuration, called a prestressable configuration. Its definition requires a brief review of a fundamental property of tensegrity structures—the prestressability property.

Prestressability of Tensegrity Structures

One of the most important properties of tensegrity structures is their prestressability. It represents their capability to attain equilibrium in the absence of external forces and torques when all tensile members (e.g., tendons) are in tension. These equilibrium configurations are called prestressable configurations and the corresponding mathematical conditions, the prestressability conditions, are given as:

$$\mathbf{A}(\mathbf{q})\mathbf{T}(\mathbf{q}) = \mathbf{0}, \qquad T_j > 0 \quad (j = 1, \ldots, 33), \tag{9}$$

where T_j is the tension in the jth working tendon.[32]

In this study, we considered a spherical prestressable configuration: all nodal points of the structure lie on the surface of the sphere (Fig. 1). Let $\mathbf{q}_0$ denote the vector of the corresponding generalized coordinates (see Appendix). The tensions in the tendons were determined by solving equation $\mathbf{A}(\mathbf{q}_0)\mathbf{T}(\mathbf{q}_0) = 0$. Because the number of columns of $\mathbf{A}(\mathbf{q}_0)$ (33) is larger than the number of rows (24) this equation has many solutions; for the present study we considered the solution for an isotropic structure in which the tendons in the 12 intermediate filaments are all equal. The tensions in all tendons are completely characterized, as shown in Appendix up to an arbitrary, positive, multiplicative scalar called the pretension coefficient or prestress, $P > 0$:

$$\mathbf{T}(\mathbf{q}_0) = P\mathbf{T}_0. \tag{10}$$

The value of $\mathbf{T}_0$ is given in Appendix. It can be seen that all tensions are positive, as required in a prestressable configuration. Note that P depends on a selection of the resting lengths l_{0j} $(j = 1, 2, \ldots, 33)$ of the working tendons. Since these are linear elastic tendons, l_{0j} and P are related by the following formula:

$$l_{0j} = \frac{l_j(\mathbf{q}_0)EA_j}{T_{0j}P + EA_j} \quad (j = 1, \ldots, 33), \tag{11}$$

where T_{0j} is the tension and $l_j(\mathbf{q}_0)$ is the length of the jth tendon corresponding to the reference solution, $\mathbf{q}_0$.

Linearized Equations of Motion

Having derived the nonlinear equations of motion (Eq. (6)) and determined a reference solution, we used the Taylor series expansion of Eq. (6) around $\mathbf{q}_0$ to obtain the corresponding linearized equations of motion. These are

$$\mathbf{C_0}\dot{\bar{\mathbf{q}}} + \mathbf{K}_0\bar{\mathbf{q}} + \mathbf{H}_0\bar{\mathbf{F}} = \mathbf{0}, \tag{12}$$

where $\bar{\mathbf{q}}$ is the perturbations vector (24×1) of independent generalized coordinates from their values at the reference solution $(\bar{\mathbf{q}} = \mathbf{q} - \mathbf{q}_0)$ and $\bar{\mathbf{F}}$ is the vector $(N \times 1)$ of perturbations in the external forces and torques $(\bar{\mathbf{F}} = \mathbf{F} - \mathbf{F}_0$, where, in this case $\mathbf{F}_0 = \mathbf{0})$. Matrices $\mathbf{C}_0$, $\mathbf{K}_0$, and $\mathbf{H}_0$ are the damping, stiffness, and disturbance matrices, respectively, evaluated at $\mathbf{q}_0$ (see Appendix for $\mathbf{H}_0$). Matrices $\mathbf{C}_0$ and $\mathbf{K}_0$ are too complicated to be given here, however, some

insight into the stiffness matrix structure is necessary for further analysis.

The stiffness matrix, $\mathbf{K}_0$, is linear in the prestress coefficient, P, and the material properties of the tendons, EA_j:

$$\mathbf{K}_0 = P\mathbf{K}_P + \sum_{j=1}^{33} EA_j\mathbf{K}_j. \tag{13}$$

Matrices $\mathbf{K}_P, \mathbf{K}_j$ (24×24) depend on the geometric properties of the structure. For frequency response calculations, an input and an output of the system have to be defined. In our study, we consider that the structure is acted upon only by an external, vertical, force, $\mathbf{F}_1 = F_1\mathbf{b}_3$, applied at the center of mass of strut B_1D_1 in Fig. 1. The magnitude component of this force, F_1, is the input to the system, and it is assumed to be small enough such that the structure undergoes small perturbations which justify the use of the linearized model to analyze its dynamic behavior through frequency response calculation. F_1 varies sinusoidally in time with the forcing frequency ω. The output is the corresponding vertical displacement in the $\mathbf{b}_3$-direction, at the point of application, Z_1. For the frequency response, the linearized output equation, which relates the output perturbation, $z_1 \equiv Z_1 - Z_{10}$ (where Z_{10} is the value of Z_1 at the reference solution, as shown in Appendix) to the generalized coordinates perturbation, $\bar{\mathbf{q}}$, is

$$z_1 = \mathbf{D}_0\bar{\mathbf{q}}, \tag{14}$$

where $\mathbf{D}_0$ is the output matrix (1×24) (see Appendix).

Frequency Response of the Model

To compare model predictions with experimental data relating to dynamic mechanical responses of cells, we transferred Eqs. (12) and (14) into the frequency domain. The transfer function, $J(\omega, P)$, between the output perturbation, z_1, and the input perturbation, F_1, was computed by applying the Laplace transform to Eqs. (12) and (14). This yielded the following equation:

$$\begin{aligned} z_1(\omega) &= -\mathbf{D}_0[\mathbf{K}_0(P) + i\omega\mathbf{C}_0]^{-1}\mathbf{H}_0F_1(\omega) \\ &= J(\omega, P)F_1(\omega), \end{aligned} \tag{15}$$

where i is the imaginary unit. The elastic (G') and frictional (G'') moduli are obtained from the following relationship:

$$J^{-1}(\omega, P) = G'(\omega, P) + iG''(\omega, P). \tag{16}$$

Note that G' and G'' are in the units of force/length. To transform these units into more traditional units, force/area, so that we can compare model predictions to experimental data, we used the equivalent continuum approximation.[27] In this approximation the work of the external force on an incremental extension per unit reference volume of the model equals the work of applied stress on an incremental change in corresponding strain (see Ref. 27 for more details). In our model, this amounts to multiplication of G' and G'' in Eq. (16) with $0.5/L$.

RESULTS

Qualitative Investigation of a Homogeneous Tensegrity Structure

We first investigated a homogeneous tensegrity model (Fig. 1) in which the material properties of all the elements are the same. Our goal was to determine whether this model that is commonly viewed as a static mechanical model could also qualitatively predict the dynamic behavior of the structure. For simplicity we assumed *ad hoc* that the stiffness of all tendons and the damping coefficients were equal to unity ($c_j = EA_j \equiv 1$), and that all struts were of unit length ($L = 1$).

In this case, the model revealed that both G' and G'' increase with increasing prestress for frequencies ranging from 0 to 10 Hz range, with G' exhibiting a greater dependence on prestress P than G'' (Fig. 2). These dependences are qualitatively similar to the ones observed in living cells in terms of their linearity.[30] Importantly, the frequency dependences of G' and G'' predicted by the model (Fig. 3) are also in general agreement with data from experimental studies with cultured mammalian cells[1,11,13]. G' has steady values at low frequencies (<1 Hz), but above 1 Hz it increases approximately linearly with frequency on the log–log scale (Fig. 3). This frequency dependence is also shifted in the direction of increasing prestress (Fig. 2). In addition, G'' exhibits an increasing dependence on frequency which is nearly linear on a log–log scale and the frequency dependence of G'' exhibits a much smaller sensitivity to prestress than in the case of G' (Fig. 3). However, the

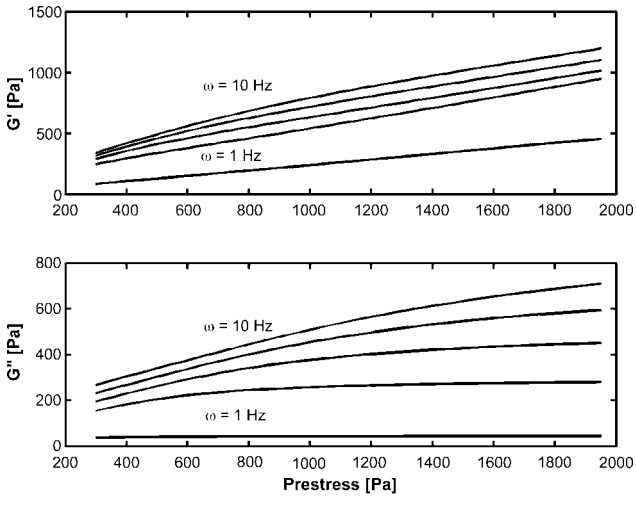

FIGURE 2. Model predictions of the elastic (G') and frictional (G'') moduli dependences on prestress for a homogeneous tensegrity structure. Each curve corresponds to a different frequency (ω) equally distributed between 1 and 10 Hz.

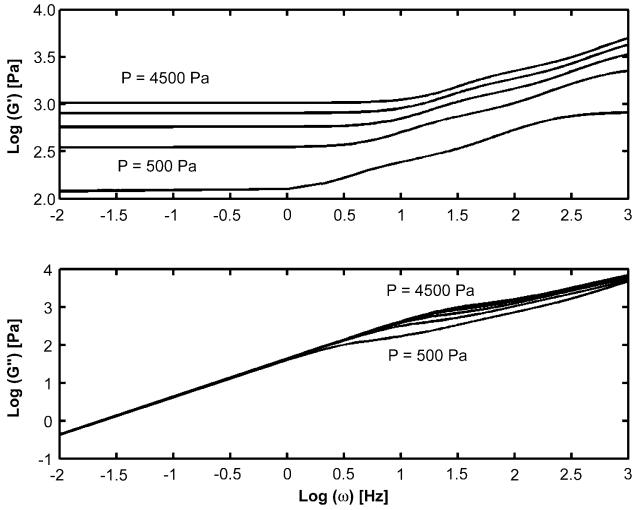

FIGURE 3. Model predictions of the elastic (*G′*) and frictional (*G″*) moduli dependences with frequency (*ω*) for a homogeneous tensegrity structure. Each curve corresponds to a different prestress (*P*) equally distributed between 500 and 4500 Pa.

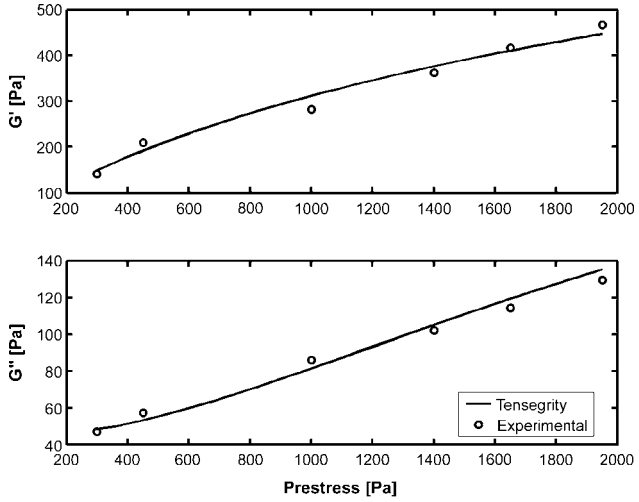

FIGURE 4. Comparison between model predictions of elastic (*G′*) and frictional (*G″*) moduli dependence on prestress for a heterogeneous tensegrity structure and the experimental results from human airway smooth muscle cells at 0.1 Hz. Circles represent experimental data replotted from Stamenović *et al.*[30]; lines indicate data generated by the tensegrity model.

dependence of G'' on frequency exhibits a log–log slope of $\sim$1 over the entire frequency range (10^{-2} to 10^{3} Hz). Experimental measurements[11] show that the slope of 1 is attained only at very high frequencies ($>10^{3}$ Hz), and that at lower frequencies this slope is an order of magnitude smaller in living cells.[11] It is noteworthy that our numerous numerical simulations carried out for different types of homogeneous tensegrity structures (e.g., various nonspherical shapes, number of elements, modules, etc.) and for different types of loading produced qualitatively similar results to those shown in Figs. 2 and 3. Thus, we conclude that homogeneous tensegrity models are capable of qualitatively matching these dynamic behaviors of living cells, but they are limited in terms of their quantitative predictions. Our numerical experiments also indicated that the frequency responses were very robust with respect to variations in the geometrical and material properties of the model. The moduli G' and G'' did not exhibit dramatic changes when the model parameters were slightly varied; for example variations of 10% in the model parameters did not result in larger than 8% variations in the moduli, indicating that the observed properties are generic and not singular phenomena.

Heterogeneous Tensegrity Structures

To further assess the quantitative capabilities of our formulation of the tensegrity model, we relaxed the homogeneity restriction and allowed the stiffness to vary between tendons. However the damping coefficient of the tendons and the length of the struts were still maintained uniform throughout the structure. Parameter values were obtained by using Matlab to numerically solve a nonlinear constrained optimization problem in which the Euclidean norm of the error between the experimental data and the results generated by the tensegrity model was minimized. The optimization parameters were the stiffnesses of the tendons, the prestress, the damping coefficient of the tendons, and the length of the struts.

Multiple solutions of the optimization problem were obtained. For example, when optimization procedure was used to fit the data for the G' and G'' versus prestress relationships at the frequency of 0.1 Hz,[30] for certain parameter values (e.g., $c = 110$, $L = 1.67$, tendon stiffness varying between 10^{-6} and 1089), the model provided a very good correspondence to the experimental data (Fig. 4). When the relationships for G' and G'' versus frequency were examined over a 5 log frequency range (10^{-2} to 10^{3} Hz), the model also provided excellent correspondence to experimental data[11] for parameter values of $L = 0.13$, damping coefficient of $c = 0.23$, prestress of $P = 0.01$, and tendon stiffness varying from 10^{-6} to 151 (Fig. 5). Our numerical simulations show that this wide distribution of the material properties is needed to match the experimental data and to simulate the wide distribution of time constants observed in living cells. The heterogeneous model also proved to be very robust with respect to variations in L, EA, and c. When these parameters values were slightly ($\sim$10%) modified from their nominal values, variations of $G'$and G'' were hardly noticeable.

DISCUSSION

Past attempts to model cell dynamic behavior have relied on *ad hoc* models (e.g., spring-dashpot models) that

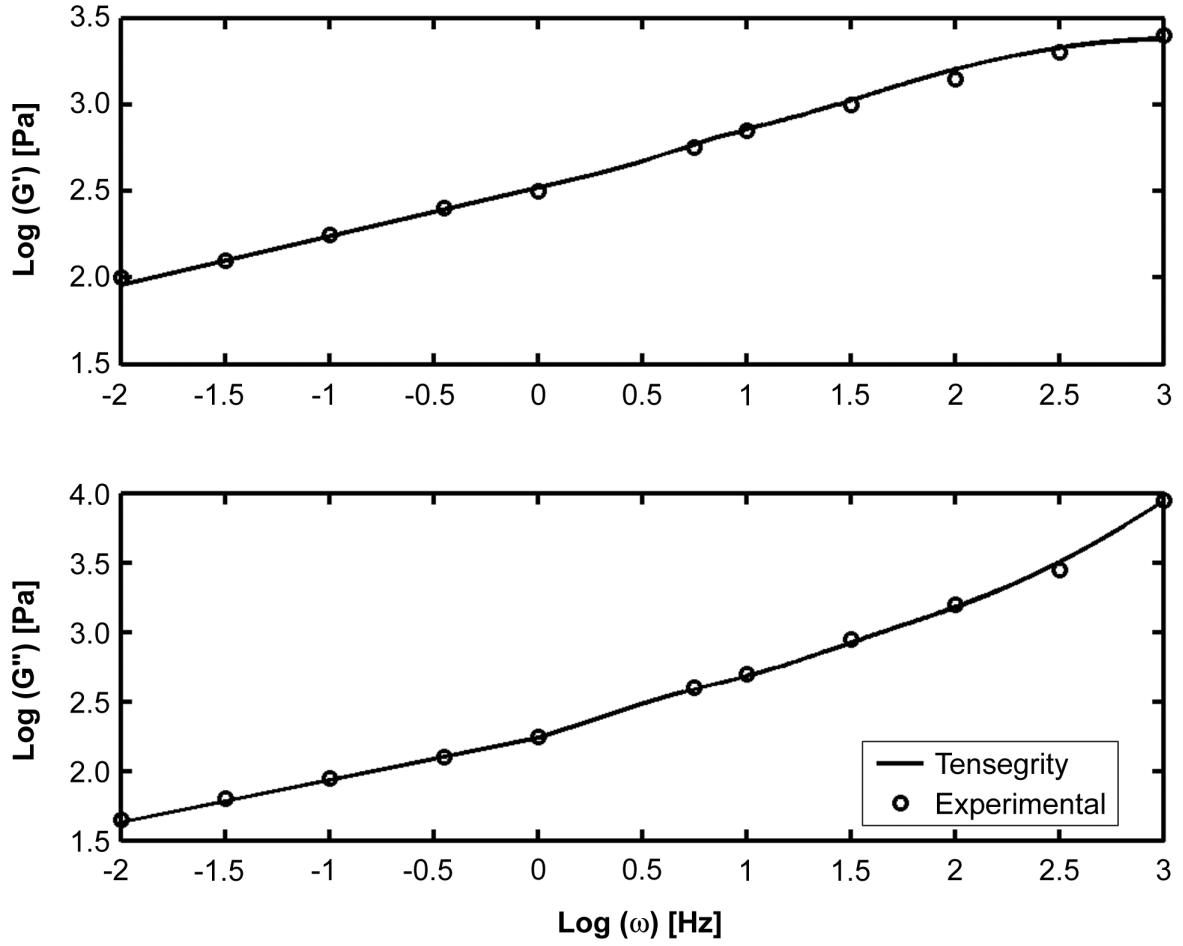

FIGURE 5. Comparison between model predictions of elastic (G') and frictional (G'') moduli dependence on frequency (ω) for a heterogeneous tensegrity structure and experimental results from human airway smooth muscle cells. Circles represent experimental data replotted from Fabry *et al.*[11]; lines indicate data generated by the tensegrity model.

are developed to fit data from specific experiments, rather than being based on knowledge of cell structure and the importance of the CSK for maintaining cell shape stability. Past formulations of the cellular tensegrity model that are based on recent insights into CSK organization have proved effective at predicting various static mechanical behaviors of living cells.[17] However, if this model embodies key features of mammalian cell mechanics, then it also should be able to predict dynamic mechanical behaviors in cells. In this study, we investigated whether the tensegrity model could also describe dynamic rheological behavior of cells. We assumed that the constitutive elements are simple, viscoelastic Voigt elements in order to find out whether a more complex behavior, that is consistent with observations in living cells, would emerge from this simple tensegrity model. We obtained results that are, in general, consistent with cell oscillatory behavior: the model provided consistent qualitative correspondence to the observed dependence of elastic and frictional moduli on both CSK prestress and the forcing frequency. However, the model failed to provide good quantitative correspondence to the experimental data under the assumption of homogeneous properties of its constituents. A good quantitative correspondence to the experimental data could be obtained only in the nonhomogeneous model in which individual cable properties differed over many orders of magnitude. Such a high variability of properties is not realistic in living cells, however. Thus, taken together, our results indicate that a simple tensegrity model may be used for qualitative description of cell dynamic behavior, but that it is limited in its current form as a quantitative model. We next critically evaluate major findings and limitations of our model.

The approximately linear dependence of G' on prestress observed in this study (Figs. 2 and 4) and past experiments with cultured cells,[30,36] has been generally attributed to various stress-supported mechanisms, including tensegrity, in the past.[28,30] However, this is the first model to effectively predict the observed dependence of G'' on prestress. In the following discussion we analyze the potential mechanisms that can explain this dependence.

The mechanisms by which stress-supported structures develop mechanical stresses to resist distortion of their shape involve changes in spacing, orientation, and length of their components.[30,31] In a purely elastic tensegrity structure that is not affected by damping and is subjected to sinusoidal external excitations, all these geometric changes are in phase and $G'' = 0$, as long as the structural response is approximately linear and resonance does not occur. However, in a tensegrity structure affected by linear damping, as is the case in this study, these changes may not all be in phase with the applied load or with each other. Since these changes depend on the prestress, the corresponding phase lags, and hence G'' also depend on the prestress.

A key assumption in our model is that damping enters the system only through the tendons, which are linearly viscoelastic Voigt elements, yielding a linearly damped system. The simple fact that the elements are viscoelastic does not necessarily imply that G'' is affected. Indeed, the system might include nonlinear viscoelastic damping and yet G'' might be 0. For example, if instead of the linear dashpots in the Voigt tendons we consider nonlinear dashpots which conform to a power-law, $\dot{l}^{\beta}$, where $\beta > 1$, the constitutive equation of each tendon, Eq. (1), becomes

$$T = EA\left(\frac{l}{l_0} - 1\right) + c\dot{l}^{\beta},$$

and the resulting linear system has a zero damping matrix, $\mathbf{C}_0 = \mathbf{0}$, yielding $G'' = 0$. This shows that rheological nonlinearities of a simple power-law type in the cables (CSK filaments) cannot explain the observed dependence of G'' on prestress. In the case when $0 < \beta < 1$, linearization is not theoretically possible, however, in the limit, approximation methods also lead to $G'' = 0$. Thus, tendons must have a linear viscous damping ($\beta = 1$) in order that $G'' > 0$. This, in turn, suggests that CSK filaments may similarly exhibit linear viscoelastic behavior in living cells in the first approximation (i.e., if the cell is subjected to small perturbations). There are no experimental data on the viscoelasticity of isolated actin filament, microtubule, or intermediate filament polymers. However, viscoelastic behavior has been observed during *in vitro* rheological measurements of reconstituted gels and suspensions containing these CSK polymers.[3,19,21] Some of these studies suggest that suspensions of actin and microtubules may conform to a weak power-law.[3] It is noteworthy that static measurements of elastic properties of isolated actin filaments indicate that they behave as linear (i.e., Hookean) springs in tension; the stiffness of these filaments remains constant over a wide range of applied tensile strains,[20] thus supporting our assumption of the elastic linearity of tendon elements in the tensegrity model.

One potential limitation of our model is that we did not consider the influence of cytoplasmic viscosity. However, the reality is that experiments with living cells show that the contribution of cytoplasmic viscosity is small at frequencies less than 10 Hz.[11] Moreover, cytoplasmic viscosity alone cannot explain the observed dependency of G'' on prestress because in general viscosity does not depend on the pressure in the liquid. Past studies also have demonstrated that cells exhibit similar mechanical behavior after membrane integrity is compromised, and hence even after cytoplasmic fluid contents are released.[35]

Another assumption in this study was that the CSK struts (e.g., microtubules) are rigid. This assumption has been introduced to obtain simpler equations of motion. The reality is that microtubules are known to buckle under compression,[36,38] and their flexibility contributes to cell deformability.[5,30] Moreover, tensegrity models that incorporate semiflexible struts are much more effective at predicting cell static behaviors than models with rigid struts.[5,6] Thus, replacement of the rigid struts with elastic elements in this model in the future may further strengthen our model.

Our numerous simulations with various homogeneous tensegrity structures could not predict the observed frequency dependence of G'' at low frequency. Specifically, the slope predicted by the homogeneous tensegrity model was an order of magnitude higher than that measured in experiments with living cells. Again, the reality is that cells are not homogeneous structures, in fact, they characteristically exhibit anisotropic structures within their CSK that result in heterogeneous force transmission throughout the cell.[14,15] When we relaxed the homogeneity assumption and allowed for the material properties of the tendons to differ as they do in living cells, the model led to effective quantitative, as well as qualitative, predictions. We note that the quantitative predictions were obtained with structures with a very high degree of heterogeneity (i.e., there was a wide range of tendons stiffnesses) which is not realistic in living cells. However one may obtain quantitative predictions with more compact distributions of the material properties, because the optimization problem to be solved in order to match the experimental data is highly nonlinear and has multiple solutions.

Several remarks are in order regarding the importance of intermediate filaments (i.e., the radial cables in Fig. 1) which were absent from the past tensegrity model used to analyze creep behavior of the cell.[4] If intermediate filaments are removed from the homogeneous tensegrity structure, the G'' versus frequency dependence exhibits a peak. Moreover, similar results were obtained for various reference configurations (e.g., for cylindrical solutions in which the nodal points of the structure lie on the surface of a rectangular cylinder) or for more complex structures composed of more elements. However, the dependences of G'' on prestress and of G' on the frequency were not dramatically affected by removing the intermediate filaments. This suggests the importance of including the radial elements that mimic the intermediate filaments into the tensegrity model. Several experimental facts are consistent with this observation. For example, disruption of intermediate filaments

caused only minor changes in the dependencies of G' and G'' on prestress.[30] This, in turn, led to the conclusion that intermediate filaments are not important for determining the dynamic behavior of cells.[30] However the intermediate filaments are known sources of nonlinear elastic behavior.[19,21] Hence further improvement of the model requires a nonlinear, non-Hookean model, for the intermediate filaments to be taken into consideration.

Another limitation of our model is the fact that it does not include mechanical contributions from other structures, such as membranes or the nucleus, or from dynamic changes in filament structure (e.g., polymerization/depolymerization, cross-link turnover). Several studies indicate that the contribution of membrane forces to resisting cell deformation is minimal.[35] For small deformations of the cell surface, the central nucleus also likely does not contribute significantly to cell mechanics; however, as the nucleus appears to be stiffer than the surrounding CSK, it may significantly impact mechanical responses to larger deformations.[23] Thus, incorporation of a nucleus with relevant material properties into a future embodiment of the tensegrity model presented here could strengthen the model.

Another potential limitation is the contribution of dynamic changes in CSK filament polymerization that may proceed on the order of seconds to minutes. However, the reality is that most major load-bearing structures in the CSK are large bundles composed of multiple filaments oriented in parallel (e.g., actin stress fibers, intermediate filament bundles). The rapid dynamics of these filaments observed in experiments with fluorescently labeled CSK monomers does not correspond to complete disruption of the CSK bundle or loss of its mechanical integrity, because it is only the external filaments at periphery of the bundle that undergo disassembly and reassembly. For this reason, the core filaments of actin stress fibers that connect to integrins within focal adhesions can maintain mechanical continuity between the cytoskeleton and extracellular matrix for periods of 15 min or more, even though adhesive contacts along the periphery of the same focal adhesion can disassemble (and reassemble) within seconds to minutes when mechanically stressed.[7] In the case of microtubules, individual filaments can either depolymerize or polymerize (shorten or lengthen) over a period of minutes. However, this usually only relates to a small subpopulation of these filaments, and the net amount of tubulin polymer (strut) remains constant in the cell.

Finally, we address the question of how important is the linearization process used in the mathematical calculations and how realistic is the assumption that the cell's behavior is largely linear during the types of experiments we describe here. A nonlinear system's dynamics is very complex and, in response to a sinusoidal excitation, the system might exhibit phenomena which are not captured by its linear approximation (e.g., subharmonics, beats, jumps, bifurcations, chaotic dynamics). None of these phenomena have been reported in the experimental papers to which our computational work has been compared.[11,13,31] Rather the behavior of the cell types used in these experiments, which employed different measurement techniques, appeared to be linear.

In summary, our results show that a tensegrity model of the CSK that incorporates a prestressed network of interconnected structural members that correspond to microfilaments, microtubules, and intermediate filaments can effectively predict dynamic mechanical properties of living mammalian cells. However, this model cannot provide good quantitative predictions of the cell behavior unless a highly nonhomogeneous distribution of structural element properties, which is not very realistic in the cell, is assumed. This, in turn, suggests that the simple tensegrity model described here is not sufficient for describing all facets of cellular dynamic behavior. Nevertheless, the model still can be greatly improved in a number of ways. In particular, future models should explore the effects of incorporating compression elements that are semiflexible, rather than rigid. They also should better convey the anisotropy, multimodularity, and heterogeneity of the cytoskeleton observed in living cells.[17] Furthermore, molecular dynamics of cytoskeletal filaments needs to be incorporated into the tensegrity model in order to obtain a more realistic description of the cell dynamic behavior. Despite its limitations, this highly simplified architecture apparently embodies the fundamental features of the cell mechanics, such as the effect of the prestress that governs the mechanical behavior of the cell.

ACKNOWLEDGMENTS

This work was supported by grants from NASA (NAG-2-1501 to D.E.I.) and NIH (HL-33009 to D.S.).

APPENDIX

The generalized coordinates at the reference solutions used in this paper can be parameterized by two angles, α and δ, being given by

$$\mathbf{q}_0 = [\delta\,\alpha\,\delta\,\alpha + 240\delta\,\alpha + 120\,X_{10}\,Y_{10}\,Z_{10}\,\delta\,\alpha + 120\,X_{20}\,Y_{20}\,Z_{20}\,\delta\,\alpha\,X_{30}\,Y_{30}\,Z_{30}\,\delta\,\alpha + 240\,X_0\,Y_0\,Z_0]^T,$$

where

$$X_{10} = -L\frac{\sqrt{6}}{8} + \frac{L}{4}\sin\delta\,\cos\alpha + L\frac{\sqrt{3}}{4}\sin\delta\,\sin\alpha,$$

$$Y_{10} = L\frac{\sqrt{2}}{8} + \frac{L}{4}\sin\alpha\,\sin\delta - L\frac{\sqrt{3}}{4}\sin\delta\,\cos\alpha,$$

$$X_{20} = L\frac{\sqrt{6}}{8} - \frac{L}{2}\sin\delta\,\cos\alpha,$$

$$Y_{20} = L\frac{\sqrt{2}}{8} - \frac{L}{2}\sin\alpha\,\sin\delta,$$

$$X_{30} = \frac{L}{4}\sin\delta\,\cos\alpha - L\frac{\sqrt{3}}{4}\sin\alpha\,\sin\delta,$$

$$Y_{30} = -L\frac{\sqrt{2}}{4} + \frac{L}{4}\,\sin\alpha\,\sin\delta + L\frac{\sqrt{3}}{4}\,\sin\delta\,\cos\alpha,$$

$$Z_{10} = Z_{20} = Z_{30} = \frac{3}{2}L\,\cos\delta - h,$$

$$X_0 = Y_0 = 0, \qquad Z_0 = L\,\cos\delta - \frac{h}{2},$$

with h given by

$$h = \frac{L}{\cos\delta}\left[\cos 2\delta + \frac{\sqrt{2}}{2}\,\sin\delta\,\cos(\alpha - 30)\right].$$

In this paper, we considered $\alpha = 60^\circ$, $\delta = 54^\circ$.

For the characterization of the vector of basis tensions, $\mathbf{T}_0$, the set of 33 active tendons is divided in five classes as follows. The intermediate filaments (I) class, which consists of 12 tendons connected to the center of the sphere. The saddle (S) tendons class consists of the six tendons connecting the B_1, B_2, B_3, C_1, C_2, and C_3 points in Fig. 1. The top (T) tendons class consists of the three tendons connecting points D_1, D_2, and D_3. The diagonal (D) tendons class consists of the following six tendons: A_1B_1, A_2B_2, A_3B_3, D_1C_3, D_2C_1, and D_3C_2. The vertical (V) tendons class consists of the following six tendons: A_1C_3, A_2C_1, A_3C_2, D_1B_3, D_2B_1, and D_3B_2.

At the reference solutions, the tensions in each class are equal and the basis tensions have the following values:

$$\mathbf{T}_0^S = 0.210, \mathbf{T}_0^V = 0.219, \mathbf{T}_0^D = 0.226,$$
$$\mathbf{T}_0^T = 0.213, \mathbf{T}_0^I = 0.022.$$

The matrix $\mathbf{H}_0$ is

$$\mathbf{H}_0 = [0\,0\,0\,0\,0\,0\,0\,0\,0\,0\,0\,0\,0\,0\,0\,0\,0\,0\,0\,1\,0\,0\,0\,0\,0]^T$$

The output matrix is

$$\mathbf{D}_0 = [0\,0\,0\,0\,0\,0\,0\,0\,0\,0\,0\,0\,0\,0\,0\,0\,0\,0\,0\,1\,0\,0\,0\,0\,0]^T.$$

REFERENCES

[1] Alcaraz, J., L. Buscemi, M. Grabulosa, X. Trepat, B. Fabry, R. Farre, and D. Navajas. Microrheology of human lung epithelial cells measured by atomic force microscopy. *Biophys. J.* 84:2071–2079, 2003.

[2] Bausch, A. R., F. Ziemann, A. A. Boulbitch, K. Jacobson, and E. Sackman. Local measurements of viscoelastic parameters of adherent cell surfaces by magnetic bead microrheometry. *Biophys. J.* 75:2038–2049, 1998.

[3] Buxbaum, R. E., T. Dennerll, S. Weiss, and S. R. Heidemann. F-actin and microtubule suspensions as indeterminate fluids. *Science* 235:1511–1514, 1987.

[4] Cañadas, P. V., M. Laurent, C. Oddou, D. Isabey, and S. Wendling. A cellular tensegrity model to analyze the structural viscoelasticity of the cytoskeleton. *J. Theor. Biol.* 218:155–173, 2002.

[5] Coughlin, M. F., and D. Stamenović. A tensegrity structure with buckling compression elements: Application to cell mechanics. *ASME J. Appl. Mech.* 64:480–486, 1997.

[6] Coughlin, M. F., and D. Stamenović. A tensegrity model of the cytoskeleton in spread and round cells. *ASME J. Biomech. Eng.* 120:770–777, 1998.

[7] Davies, P. F., A. Robotewskyj, and M. L. Griem. Directional remodeling of focal adhesion sites in response to flow forces. *J. Clin. Invest.* 93:2031–2038, 1994.

[8] Davies, P. F., and S. C. Tripathi. Mechanical stress mechanisms and the cell: An endothelial paradigm. *Circ. Res.* 72:239–245, 1993.

[9] Elson, E. L. Cellular mechanics as an indicator of cytoskeletal structure and function. In: Annual Review of Biophysics and Biophysical Chemistry, edited by D. M. Engleman, C. R. Cantor, and T. D. Pollard. Palo Alto, CA: Annual Reviews Inc., 1988, pp. 397–430.

[10] Elson, E. L., B. B. Daily, W. B. McConnaughey, C. Pasternak, and N. O. Petersen. Measurement of forces which determine the shapes of adherent cells in culture. In: Frontiers in Biochemical and Biophysical Studies of Proteins and Membranes, New York: Elsevier Science, 1983, pp. 399–411.

[11] Fabry, B., G. N. Maksym, J. P. Butler, M. Glogauer, D. Navajas, and J. J. Fredberg. Scaling the microrheology of living cells. *Phys. Rev. Lett.* 87:148102, 2001.

[12] Fung, Y. C., and S. Q. Liu. Elementary mechanics of the endothelium of blood vessels. *ASME J. Biomech. Eng.* 115:1–12, 1993.

[13] Goldmann, W. H., and R. M. Ezzell. Viscoelasticity in wild type and vinculin deficient mouse F9 embryonic carcinoma cells examined by atomic force microscopy and rheology. *Exp. Cell Res.* 226:234–237, 1993.

[14] Helmke, B. P., A. B. Rosen, and P. F. Davies. Mapping mechanical strain of an endogenous cytoskeletal network in living endothelial cells. *Biophys. J.* 84:2691–2699, 2003.

[15] Hu, S., J. Chen, B. Fabry, Y. Numaguchi, A. Gouldstone, D. E. Ingber, J. J. Fredberg, J. P. Butler, and N. Wang. Intracellular stress tomography reveals stress focusing and structural anisotropy in the cytoskeleton of living cells. *Am. J. Physiol. Cell Physiol*, 285: C1082–C1090, 2000.

[16] Ingber, D. E. Cellular tensegrity: Defining new rules of biological design that govern the cytoskeleton. *J. Cell Sci.* 104:613–627, 1993.

[17] Ingber, D. E. Tensegrity I: Cell structure and hierarchical systems biology. *J. Cell Sci.* 116:1157–1173, 2003.

[18] Janmey, P. A. The cytoskeleton and cell signaling: Component localization and mechanical coupling. *Physiol. Rev.* 78:763–781, 1998.

[19] Janmey, P. A., U. Eutenauer, P. Traub, and M. Schliwa. Viscoelastic properties of vimentin compared with other filamentous biopolymer networks. *J. Cell Biol.* 113:155–160, 1991.

[20] Kojima, H., A. Ishijima, and T. Yanagida. Direct measurement of stiffness of single actin filaments with and without tropomyosin by in vitro nanomanipulation. *Proc. Natl. Acad. Sci. U.S.A.* 91:12962–12966, 1994.

[21] Ma, L., J. Xu, P. A. Coulombe, and D. Wirtz. Keratin filament suspensions show unique micromechanical properties. *J. Biol. Chem.* 274:19145–19151, 1999.

[22] Maksym, G. N., B. Fabry, J. Laporte, P. E. Moore, J. P. Butler, D. Navajas, and J. J. Fredberg. Mechanical properties of cultured human airway smooth muscle cells from 0.05 to 0.4 Hz. *J. Appl. Physiol.* 89:1619–1632, 2000.

[23] Maniotis, A. J., C. S. Chen, and D. E. Ingber. Demonstration of mechanical connections between integrins, cytoskeletal filaments, and nucleoplasm that stabilize nuclear structure. *Proc. Natl. Acad. Sci. U.S.A.* 94:849–854, 1997.

[24] Satcher, R. L., Jr., and C. F. Dewey Jr. Theoretical estimates of mechanical properties of the endothelial cell cytoskeleton. *Biophys. J.* 71:109–118, 1996.

[25]Sato, M., D. P. Theret, L. T. Wheeler, N. Oshima, and R. M. Nerem. Application of the micropipette technique to the measurements of cultured porcine aortic endothelial cell viscoelastic properties. *ASME J. Biomech. Eng.* 112:263–268, 1990.

[26]Shroff, S. G., D. R. Saner, and R. Lal. Dynamic micromechanical properties of cultured rat arterial myocytes measured by atomic force microscopy. *Am. J. Physiol. Cell Physiol.* 269:C268–C292, 1995.

[27]Stamenović, D., and M. F. Coughlin. The role of prestress and architecture of the cytoskeleton and deformability of cytoskeletal filaments in mechanics of adherent cells; a quantitative analysis. *J. Theor. Biol.* 201:63–74, 1999.

[28]Stamenović, D., and M. F. Coughlin. A quantitative model of cellular elasticity based on tensegrity. *ASME J. Biomech. Eng.*122:39–43, 2000.

[29]Stamenović, D., J. J. Fredberg, N. Wang, J. P. Butler, and D. E. Ingber. A microstructural approach to cytoskeletal mechanics based on tensegrity. *J. Theor. Biol*. 181:125–136, 1996.

[30]Stamenović, D., Z. Liang, J. Chen, and N. Wang. The effect of the cytoskeletal prestress on the mechanical impedance of cultures airway smooth muscle cells. *J. Appl. Physiol.* 92:1443–1450, 2002.

[31]Stamenović, D., and N. Wang. Cellular responses to mechanical stress: Engineering approaches to cytoskeletal mechanics. *J. Appl. Physiol.* 89:2085–2090, 2000.

[32]Sultan, C., M. Corless, and R. E. Skelton. The prestressability problem of tensegrity structures. Some analytical solutions. *Intl. J. Solids Struct.* 38:5223–5252, 2001.

[33]Thoumine, O., and A. Ott. Time scale dependent viscoelastic and contractile regimes in fibroblasts probed by microplate manipulation. *J. Cell Sci.* 110:2109–2116, 1997.

[34]Wang, N., J. P. Butler, and D. E. Ingber. Mechanotransduction across the cell surface and through the cytoskeleton. *Science* 260:1124–1127, 1993.

[35]Wang, N., and D. E. Ingber. Control of cytoskeletal mechanics by extracellular matrix, cell shape, and mechanical tension. *Biophys. J.* 66:2181–2189, 1994.

[36]Wang, N., K. Naruse, D. Stamenović, J. J. Fredberg, S. M. Mijailovich, I. M. Tolić-Nørrelykke, T. Polte, R. Mannix, and D. E. Ingber. Mechanical behavior in living cells consistent with the tensegrity model. *Proc. Natl. Acad. Sci. U.S.A.* 98:7765–7770, 2001.

[37]Wang, N., and D. Stamenović. Contribution of intermediate filaments to cell stiffness, stiffening, and growth. *Am. J. Physiol. Cell Physiol.* 279:C188–C194, 2000.

[38]Waterman-Storer, C. M., and E. D. Salmon. Actomyosin-based retrograde flow of microtubules in the lamella of migrating epithelial cells influences microtubule dynamic stability and turnover is associated with microtubule breakage and treadmilling. *J. Cell Biol*. 139:417–434, 1997.

[39]Wendling, S., C. Oddou, and D. Isabey. Stiffening response of a cellular tensegrity model. *J. Theor. Biol.* 196:309–325, 1999.

[40]Yeung, A., and E. Evans. Cortical shell-liquid core model for passive flow of liquid-like spherical cells into micropipettes. *Biophys. J.* 56:139–149, 1989.